Inorg. Chem. **2006**, *45*, 10790–10798

Synthesis, Structure, and ^{15}N NMR Studies of Paramagnetic Lanthanide Complexes Obtained by Reduction of Dinitrogen

William J. Evans,* Daniel B. Rego, and Joseph W. Ziller

Department of Chemistry, University of California, Irvine, California 92697-2025

Received August 7, 2006

The recently discovered LnZ_3/M and LnZ_2Z'/M methods of reduction (Ln = lanthanide; M = alkali metal; Z, Z′ = monoanionic ligands that allow these combinantions to generate "LnZ_2" reactivity) have been applied to provide the first crystallographically characterized dinitrogen complexes of cerium, $[(C_5Me_5)_2(THF)Ce]_2(\mu\text{-}\eta^2\text{:}\eta^2\text{-}N_2)$ and $[(C_5Me_4H)_2(THF)Ce]_2(\mu\text{-}\eta^2\text{:}\eta^2\text{-}N_2)$, so that the utility of ^{15}N NMR spectroscopy with paramagnetic lanthanides could be determined. $[(C_5Me_5)_2(THF)Pr]_2(\mu\text{-}\eta^2\text{:}\eta^2\text{-}N_2)$ and $[(C_5Me_4H)_2(THF)Pr]_2(\mu\text{-}\eta^2\text{:}\eta^2\text{-}N_2)$ were also synthesized, crystallographically characterized, and studied by ^{15}N NMR methods. The data were compared to those of $[(C_5Me_5)_2Sm]_2(\mu\text{-}\eta^2\text{:}\eta^2\text{-}N_2)$. $[(C_5Me_5)_2(THF)Ce]_2(\mu\text{-}\eta^2\text{:}\eta^2\text{-}N_2)$ and $[(C_5Me_5)_2(THF)Pr]_2(\mu\text{-}\eta^2\text{:}\eta^2\text{-}N_2)$ are unlike their $(C_5Me_4H)^{1-}$ analogs in that the solvating THF molecules are cis rather than trans. Structural information on precursors, $(C_5Me_4H)_3Ce$, $(C_5Me_4H)_3Pr$, and the oxidation product $[(C_5Me_5)_2Ce]_2(\mu\text{-}O)$ is also presented.

Introduction

Although ^{15}N NMR spectroscopy is used extensively to study dinitrogen reduction in diamagnetic metal systems,[1−7] no spectra have been reported, to our knowledge, on any of the dinitrogen complexes of the paramagnetic lanthanides.[1−8] Since most of the lanthanide ions are paramagnetic and numerous paramagnetic lanthanide dinitrogen complexes have been synthesized, it was of interest to determine if ^{15}N NMR spectroscopy could be used to characterize these complexes.

The paramagnetic Ln^{3+} ions most desirable for initial study are those with the smallest magnetic moments, namely the elements at the beginning of the series, Ce−Sm, where orbital and spin angular momentum are in opposition. Sm^{3+} (μ = 0.84 μ_B)[9] has the lowest magnetic susceptibility of these ions, but analysis of the dinitrogen complex of this ion, $[(C_5Me_5)_2Sm]_2(\mu\text{-}\eta^2\text{:}\eta^2\text{-}N_2)$,[10] **1**, is complicated because the complex forms an equilibrium with its Sm^{2+} precursor, eq 1. The ions with the next lowest moments are $4f^1$ Ce^{3+} (μ = 2.54 μ_B)[9]

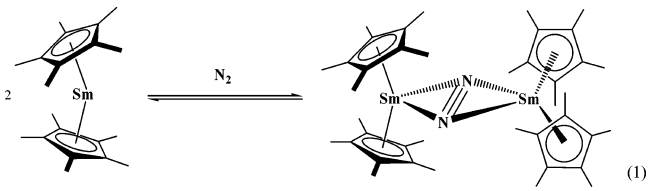

(1)

and $4f^4$ Pm^{3+} (μ = 2.68 μ_B).[9] Since the latter is radioactive, cerium was the best target for study. Unfortunately, Ce^{3+} was one of the ions that did not give crystallizable dinitrogen complexes in the earlier study of LnZ_3/K reactions in which Z = $[N(SiMe_3)_2]^{1-}$,[4] eq 2.

To obtain cerium dinitrogen complexes for ^{15}N NMR studies and to demonstrate that crystallographically characterizable dinitrogen complexes could be isolated for cerium,

* To whom correspondence should be addressed. E-mail: wevans@uci.edu.

(1) (a) Einsle, O.; Tezcan, F. A.; Andreade, S. L. A.; Schmid, B.; Yoshida, M.; Howard, J. B.; Rees, D. C. *Science* **2002**, *297*, 1696. (b) Lee, S. C.; Holm, R. H. *Proc. Natl. Acad. Sci. U.S.A.* **2003**, *100*, 3595. (c) Dubé, T.; Ganesan, M.; Conoci, S.; Gambarotta, S.; Yap, G. P. A. *Organometallics* **2000**, *19*, 3716. (d) Roussekm, O.; Errington, W.; Kaltsoyannis, N.; Scott, P. *J. Organomet. Chem.* **2001**, *635*, 69. (e) Sanner, R. D.; Manriquez, J. M.; Marsh, R. E.; Bercaw, J. E. *J. Am. Chem. Soc.* **1976**, *98*, 8351. (f) Fryzuk, M. D.; Haddad, T. S.; Rettig, S. J. *J. Am. Chem. Soc.* **1990**, *112*, 8185. (g) Pool, J. A.; Lobkovsky, E.; Chirik, P. J. *Nature (London)* **2004**, *427*, 527.
(2) von Philipsborn, W.; Müller, R. *Angew. Chem., Int. Ed. Engl.* **1986**, *25*, 383.
(3) Evans, W. J.; Lee, D. S.; Ziller, J. W. *J. Am. Chem. Soc.* **2004**, *126*, 454.
(4) Evans, W. J.; Lee, D. S.; Rego, D. B.; Perotti, J. M.; Kozimor, S. A.; Moore, E. K.; Ziller, J. W. *J. Am. Chem. Soc.* **2004**, *126*, 14574.
(5) Evans, W. J.; Lee, D. S.; Lie, C.; Ziller, J. W. *Angew. Chem., Int. Ed.* **2004**, *43*, 5517.
(6) Evans, W. J.; Lee, D. S.; Johnston, M. A.; Ziller, J. W. *Organometallics* **2005**, *24*, 6393.
(7) Evans, W. J.; Lee, D. S. *Can. J. Chem.* **2005**, *83*, 375.
(8) MacLachlan, E. A.; Fryzuk, M. D. *Organometallics* **2006**, *25*, 1530.
(9) Emeléus, H. J.; Sharpe A. G. *Modern Aspects of Inorganic Chemistry*, 4th ed.; John Wiley and Sons: New York, 1973; p l481.
(10) Evans, W. J.; Ulibarri, T. A.; Ziller, J. W. *J. Am. Chem. Soc.* **1988**, *110*, 6877.

10.1021/ic061485g CCC: $33.50
Published on Web 12/02/2006

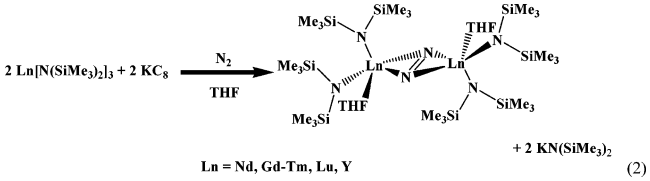

(2)

the LnZ_3/K and LnZ_2Z'/K reduction methods[3−7] were applied to cerium using $Z = (C_5Me_5)^{1-}$ and $(C_5Me_4H)^{1-}$ and $Z' = (BPh_4)^{1-}$. This method was also applied to the praseodymium analogs to obtain another pair of paramagnetic dinitrogen complexes with low magnetic moments ($4f^2$ Pr^{3+}, $\mu = 3.58$ μ_B[9]). With these data in hand for comparison, variable-temperature ^{15}N studies were conducted on the equilibrium in eq 1.

Experimental Section

The manipulations described below were performed under nitrogen with the rigorous exclusion of air and water using Schlenk, vacuum line, and glovebox techniques. $[(C_5Me_5)_2Ln][(\mu\text{-}Ph)_2BPh_2]$ (Ln= Ce, Pr),[11] $(C_5Me_5)_2Sm$,[12] and KC_8[13] were made according to the literature. $^{15}N_2$ was purchased from Cambridge Isotope Laboratories and used as received. Hydrated lanthanide trichlorides were desolvated with NH_4Cl.[14] C_5Me_5H was dried over molecular sieves and degassed prior to use. $C_5Me_4H_2$ was distilled onto molecular sieves and degassed prior to use. KC_5Me_5 and KC_5Me_4H were prepared by adding C_5Me_5H and $C_5Me_4H_2$, respectively, to excess potassium bis(trimethylsilyl)amide or potassium bis(dimethylphenylsilyl)amide[15] in toluene. Solvents were sparged with argon and dried as previously described.[15] Magnetic susceptibility was determined according to the literature.[16] NMR solvents were dried over sodium potassium alloy, degassed, and vacuum-transferred before use. ^1H and ^{13}C NMR spectra were recorded on a Bruker GN 500 MHz spectrometer. ^{15}N NMR spectra were obtained with Bruker GN 500 MHz and Bruker Advance 600 MHz spectrometers. ^{15}N NMR spectra were measured using an external reference of ^{15}N-formamide (δ −267.8 with respect to nitromethane at δ 0).[17] Infrared spectra were recorded as thin films obtained from either benzene or THF using an ASI ReactIR 1000 spectrometer.[18] Elemental analyses were performed by complexometric titration.[19]

$[(C_5Me_5)_2Sm]_2(\mu\text{-}\eta^2\text{:}\eta^2\text{-}^{15}N_2)$, 1. A concentrated solution of $(C_5Me_5)_2Sm$ in ca. 1 mL of d_8-toluene in a J-Young NMR tube was degassed by three freeze−pump−thaw cycles and the solution was exposed to 1 atm of $^{15}N_2$. ^{15}N NMR (C_7D_8) at 263 K, δ −117; 248 K, δ −125; 233 K, δ −135; 218 K, δ −146; 203 K, δ −161.

Synthesis of $[(C_5Me_5)_2(THF)Ce]_2(\mu\text{-}\eta^2\text{:}\eta^2\text{-}N_2)$, 2. In a glovebox, $[(C_5Me_5)_2Ce][(\mu\text{-}Ph)_2BPh_2]$ (136 mg, 0.16 mmol) was added to KC_8 (37 mg, 0.27 mmol) in 10 mL of THF, and the mixture was stirred for 2 h. The solution was centrifuged to remove white and black solids, and the solvent was removed in vacuo. Toluene extraction followed by centrifugation and removal of solvent from the supernatant in vacuo left a dark red oil. Recrystallization from toluene gave dark red needles of **2** (60 mg, 74%). $\chi_M^{298K} = 1459 \times 10^{-6}$ (cgs); $\mu_{eff} = 1.9$ μ_B. ^1H NMR (C_7D_8) δ −0.46 (8H, *THF*), −0.03 (8H, *THF*), 1.17 (60H, C_5Me_5). ^{13}C NMR (C_7D_8) δ 4.3 (C_5Me_5), 22.0 (*THF*), 53.8 (*THF*), 159.4 (C_5Me_5). ^{15}N NMR (C_7D_8) δ 871 (fwhh 22 Hz[20]). Anal. Calcd for $C_{48}H_{76}N_2O_2Ce_2$: Ce, 28.21. Found: Ce, 27.7. IR (C_6H_6) 3667w, 3640w, 3034w, 2957s, 2907vs, 2856vs, 2725w, 2362w, 2342w, 2142w, 1552s, 1494w, 1440vs, 1378s, 1258w, 1189 m, 1058 m, 1023s, 973 m, 872w, 803 m, 730 m, 710 m, 676vs, 587s cm^{-1}.

Synthesis of $[(C_5Me_5)_2(THF)Pr]_2(\mu\text{-}\eta^2\text{:}\eta^2\text{-}N_2)$, 3. Following the procedure for **2,** $[(C_5Me_5)_2Pr][(\mu\text{-}Ph)_2BPh_2]$ (202 mg, 0.24 mmol) was added to KC_8 (43 mg, 0.31 mmol) in 10 mL of THF. Recrystallization from toluene gave dark orange needles (103 mg, 85%). $\chi_M^{298K} = 4358 \times 10^{-6}$ (cgs); $\mu_{eff} = 3.2$ μ_B. ^1H NMR (C_7D_8) δ 2.73 (C_5Me_5), THF resonances could not be located. ^{13}C NMR (C_7D_8) δ −10.21 (C_5Me_5), 210.9 (C_5Me_5), THF resonances could not be located. ^{15}N NMR (C_7D_8) δ 2231 (fwhh 93 Hz[20]). Anal. Calcd for $C_{48}H_{76}N_2O_2Pr_2$: Pr, 28.27. Found: Pr, 28.9. IR (THF) 3675w, 3640w, 2971s, 2907s, 2856s, 2725w, 2362w, 2343w, 1969w, 1660w, 1610w, 1567w, 1536w, 1598w, 1447 m, 1378w, 1312w, 1289w, 1239w, 1208 m, 1181 m, 1104 m, 1069vs, 1031 m, 988w, 911s, 733w, 714w, 664w cm^{-1}.

Synthesis of $(C_5Me_4H)_3Ce$, 4. Similar to the method of Schumann, et al.,[21,22] $CeCl_3$ (280 mg, 1.14 mmol) and KC_5Me_4H (548 mg, 3.42 mmol) were combined in 100 mL of THF and allowed to stir overnight. The solution was filtered, and the solvent was removed from the solution in vacuo. Toluene extraction followed by filtering and removal of the solvent in vacuo left a green powder (448 mg, 85%). ^1H NMR (C_6D_6) δ −10.88 (18H, C_5Me_4H), 7.82 (18H, C_5Me_4H), 33.56 (3H, C_5Me_4H). ^{13}C NMR (C_6D_6) δ −11.6 (C_5Me_5H), 15.9 (C_5Me_4H), 158.9 (C_5Me_4H), 176.8 (C_5Me_4H), 198.4 (C_5Me_4H). Anal. Calcd for $C_{27}H_{39}Ce$: Ce, 27.81. Found: Ce, 27.4.

Synthesis of $(C_5Me_4H)_3Pr$, 5. Following the procedure for **4**, $PrCl_3$ (402 mg, 1.63 mmol) and KC_5Me_4H (766 mg, 4.84 mmol) gave a yellow powder. (0.640 g, 78%). ^1H NMR (C_6D_6) δ −30.5 (18H, C_5Me_4H), 19.0 (18H, C_5Me_4H), 78.2 (3H, C_5Me_4H). ^{13}C NMR (C_6D_6) δ −49.3 (C_5Me_4H), 15.8 (C_5Me_4H), 251.3 (C_5Me_4H), 280.4 (C_5Me_4H), 328.8 (C_5Me_4H). Anal. Calcd for $C_{27}H_{39}Pr$: Pr, 27.93. Found: Pr, 27.6.

Synthesis of $[(C_5Me_4H)_2(THF)Ce]_2(\mu\text{-}\eta^2\text{:}\eta^2\text{-}N_2)$, 6. In a glovebox, complex **4** (68 mg, 0.13 mmol) was added to KC_8 (20 mg, 0.15 mmol) in 10 mL of THF. The solution became red and was allowed to stir for 3 h. The solution was centrifuged, and the solvent was removed from the supernatant in vacuo to give dark red solids. Toluene extraction, followed by centrifugation and removal of solvent from the supernatant in vacuo, left a yellow-green oil. Yellow crystals were obtained from toluene at −35 °C (45 mg, 71%). Complex **6** was obtained similarly from reaction of **4** and either excess K or excess Na. ^1H NMR (C_7D_8) δ −4.16, −0.31, 0.80, 1.63, 11.80. ^{13}C NMR (C_7D_8) δ 0.9, 1.5, 14.2. ^{15}N NMR

(11) Evans, W. J.; Perotti, J. M.; Kozimor, S. A.; Champagne, T. M.; Davis, B. L.; Nyce, G. W.; Fujimoto, C. H.; Clark, T. D.; Johnston, M. A.; Ziller, J. W. *Organometallics* **2005**, *24*, 2916.
(12) Evans, W. J.; Hughes, L. A.; Hanusa, T. P. *J. Am. Chem. Soc.* **1984**, *106*, 4270.
(13) Bergbreiter, D. E.; Killough, J. M. *J. Am. Chem. Soc.* **1978**, *100*, 2126.
(14) Taylor, M. D.; Carter, C. P. *J. Inorg. Nucl. Chem.* **1962**, *24*, 387.
(15) Evans, W. J.; Rego, D. B.; Ziller, J. W. *Inorg. Chem.* **2006**, *45*, 3437.
(16) (a) Evans, D. F. *J. Chem. Soc.* **1959**, 2003−2005. (b) Becconsal, J. K. *Mol. Phys.* **1968**, *15*, 129−139. (c) Lide, D. R., Ed. *CRC Handbook of Chemistry and Physics*, 72nd ed.; CRC Press: Boca Raton, FL, 1991−1992. (d) Shoemaker, D. P.; Garland, C. W.; Steinfeld, J. I.; Nibler, J. W. *Experiments in Physical Chemisty*, 4th ed.; McGraw-Hill, New York, 1981; p 402.
(17) (a) Buchanan, G. W.; Crutchley, R. J. *Magn. Reson. Chem.* **1994**, *32*, 552. (b) Levy, G. C.; Lichter, R. L. *Nitrogen-15 Nuclear Magnetic Resonance Spectroscopy*; Wiley-Interscience: New York, 1979.
(18) Evans, W. J.; Johnston, M. A.; Clark, R. D.; Ziller, J. W. *Inorg. Chem.* **2000**, *39*, 3421.
(19) Evans, W. J.; Engerer, S. C.; Coleson, K. M. *J. Am. Chem. Soc.* **1981**, *103*, 6672.
(20) Exponential line broadening at 10 Hz was used in the data processing.
(21) Schumann, H.; Glanz, M.; Hemling, H. *J. Organomet. Chem.* **1993**, *445*, C1.
(22) Schumann, H.; Glanz, M.; Hemling, H.; Hahn, F. E. *Z. Anorg. Allg. Chem.* **1995**, *621*, 341.

Table 1. X-ray Data Collection Parameters for $[(C_5Me_5)_2(THF)Ce]_2(\mu\text{-}\eta^2\text{:}\eta^2\text{-}N_2)$, **2**, $[(C_5Me_5)_2(THF)Pr]_2(\mu\text{-}\eta^2\text{:}\eta^2\text{-}N_2)$, **3**, $(C_5Me_4H)_3Ce$, **4**, $(C_5Me_4H)_3Pr$, **5**, $[(C_5Me_4H)_2(THF)Ce]_2(\mu\text{-}\eta^2\text{:}\eta^2\text{-}N_2)$, **6**, $[(C_5Me_4H)_2(THF)Pr]_2(\mu\text{-}\eta^2\text{:}\eta^2\text{-}N_2)$, **7**, and $[(C_5Me_5)_2Ce]_2(\mu\text{-}O)$, **8**[a]

empirical formula	$C_{48}H_{76}Ce_2N_2O_2\cdot 2(C_7H_8)$ **2**	$C_{48}H_{76}Pr_2N_2O_2\cdot 2(C_7H_8)$ **3**	$C_{27}H_{39}Ce$ **4**	$C_{27}H_{39}Pr$ **5**
fw	1177.62	1179.20	503.70	504.49
T (K)	158(2)	163(2)	163(2)	163(2)
cryst syst	monoclinic	monoclinic	rhombohedral	rhombohedral
space group	$C2/c$	$C2/c$	$R\bar{3}$	$R\bar{3}$
a (Å)	18.161(5)	18.1582(19)	15.7088(6)	15.6697(6)
b (Å)	20.026(6)	19.943(2)	15.7088(6)	15.6697(6)
c (Å)	15.861(5)	15.8519(16)	16.4763(12)	16.4894(11)
α (deg)	90	90	90	90
β (deg)	96.661(5)	97.072(2)	90	90
γ (deg)	90	90	120	120
V Å^3	5730(3)	5696.8(10)	3521.1(3)	3506.4(3)
Z	4	4	6	6
ρ_{calcd} (Mg/m^3)	1.365	1.375	1.425	1.434
μ (mm^{-1})	1.611	1.733	1.949	2.094
R1 [$I > 2.0\sigma(I)$]	0.0456	0.0451	0.0161	0.0128
wR2 (all data)	0.1318	0.1229	0.0395	0.0315

empirical formula	$C_{44}H_{68}Ce_2N_2O_2\cdot 2(C_7H_8)$ **6**	$C_{44}H_{68}Pr_2N_2O_2\cdot 2(C_7H_8)$ **7**	$C_{40}H_{60}Ce_2O$ **8**
fw	1121.51	1123.09	837.12
T (K)	163(2)	163(2)	163(2)
cryst syst	monoclinic	monoclinic	tetragonal
space group	$C2/c$	$C2$	$I\bar{4}2m$
a (Å)	15.3012(13)	15.3137(18)	11.4716(6)
b (Å)	14.1562(12)	14.1046(17)	11.4716(6)
c (Å)	25.765(2)	12.8773(15)	14.2381(15)
α (deg)	90	90	90
β (deg)	104.1150(10)	104.177(12)	90
γ (deg)	90	90	90
V Å^3	5412.4(8)	2696.7(6)	1873.7(2)
Z	4	2	2
ρ_{calcd} (Mg/m^3)	1.376	1.383	1.484
μ (mm^{-1})	1.702	1.826	2.426
R1 [$I > 2.0\sigma(I)$]	0.0370	0.0366	0.0170
wR2 (all data)	0.1001	0.0964	0.0417

[a] wR2 = $[\sum[w(F_o^2 - F_c^2)^2]/\sum[w(F_o^2)^2]\ ]^{1/2}$. R1 = $\sum||F_o| - |F_c||/\sum|F_o|$.

(C_7D_8) δ 1001 (fwhh 24 Hz[20]). Anal. Calcd for $C_{44}H_{68}N_2O_2Ce_2$: Ce, 29.90. Found: Ce, 29.0.

Synthesis of $[(C_5Me_4H)_2(THF)Pr]_2(\mu\text{-}\eta^2\text{:}\eta^2\text{-}N_2)$, 7. Following the procedure for **6**, complex **5** (54 mg, 0.11 mmol) and KC_8 (17 mg, 0.13 mmol) in 10 mL of THF gave a yellow-green oil. Dark green crystals were obtained from toluene at −35 °C (37 mg, 74%). Complex **7** was obtained similarly from reaction of **5** and either excess K or excess Na. ^{1}H NMR (C_7D_8) δ −7.8, −2.9, 6.4, 20.9. ^{13}C NMR (C_7D_8) δ −21.4, −12.4, 13.8, 35.7, 120.1. ^{15}N NMR (C_7D_8) δ 2383 (fwhh 114 Hz[20]). Anal. Calcd for $C_{44}H_{68}N_2O_2Pr_2$: Pr, 30.02. Found: Pr, 29.7.

^{15}N-Labeled Compounds. The ^{15}N-labeled analog of **2** was prepared as follows. THF (ca. 10 mL) was degassed through three consecutive freeze−pump−thaw cycles and vacuum-transferred to a reaction vessel fitted with a greaseless high-vacuum stopcock containing $[(C_5Me_5)_2Ce][BPh_4]$ (156 mg, 0.19 mmol) and KC_8 (29 mg, 0.21 mmol). $^{15}N_2$-labeled gas was admitted to the reaction system, and the mixture was stirred for ca. 2 h. The product was isolated as described for **2**. ^{15}N-labeled compounds of **3**, **6**, and **7** were prepared similarly.

X-ray Data Collection, Structure Determination, and Refinement for 2−8. X-ray crystallographic data were obtained by mounting a crystal on a glass fiber and transferring it to a Bruker CCD platform diffractometer. The SMART[23] program package was used to determine the unit-cell parameters and for data collection (45 s/frame scan time for **2**, 30 s/frame scan time for **3** and **8**, and 25 s/frame scan time for **4**−**7**; scan times were for a hemisphere of diffraction data for **2** and **8**, and for a sphere of diffraction data for **3**−**7**). The raw frame data was processed using SAINT[24] and SADABS[25] to yield the reflection data file. Subsequent calculations were carried out using the SHELXTL[26] program. The analytical scattering factors[27] for neutral atoms were used throughout the analysis. Crystallographic data appear in Table 1.

$[(C_5Me_5)_2(THF)Ce]_2(\mu\text{-}\eta^2\text{:}\eta^2\text{-}N_2)$, 2. A small red crystal of approximate dimensions 0.06 × 0.14 × 0.23 mm^3 was handled as described above. The diffraction symmetry was 2/*m*, and the systematic absences were consistent with the monoclinic space groups *Cc* and *C*2/*c*. It was later determined that the centrosymmetric space group *C*2/*c* was correct. The structure was solved using the coordinates obtained from a direct methods solution of a previous data set and refined on F^2 by full-matrix least-squares techniques. Hydrogen atoms were included using a riding model. The molecule was located about a 2-fold rotation axis. There were two molecules of toluene solvent present per formula unit. One solvent molecule was located about a 2-fold rotation axis, while

(23) *SMART Software Users Guide, Version 5.1*; Bruker Analytical X-Ray Systems, Inc.; Madison,WI, 1999.

(24) *SAINT Software Users Guide, Version 6.0*; Bruker Analytical X-Ray Systems, Inc.; Madison, WI, 1999.

(25) Sheldrick, G. M. *SADABS, Version 2.10*; Bruker Analytical X-Ray Systems, Inc.; Madison, WI, 2002.

(26) Sheldrick, G. M. *SHELXTL Version 6.12*; Bruker Analytical X-Ray Systems, Inc.; Madison, WI, 2001.

(27) *International Tables for X-Ray Crystallography*; Kluwer Academic Publishers: Dordrecht, 1992; Vol. C.

the other was located about an inversion center. Both solvent molecules were disordered and included using multiple components, partial site-occupancy factors, and geometrical restraints. Hydrogen atoms associated with the solvent molecules were not included. At convergence, wR2 = 0.1318 and GOF = 1.041 for 295 variables refined against 5845 data (0.80 Å). As a comparison for refinement on *F*, R1 = 0.0456 for those 4445 data with $I > 2.0\sigma(I)$.

[(C$_5$Me$_5$)$_2$(THF)Pr]$_2$(μ-η^2:η^2-N$_2$), 3. A yellow-orange crystal of approximate dimensions 0.08 × 0.10 × 0.20 mm^3 was handled as described above. The diffraction symmetry was 2/*m*, and the systematic absences were consistent with the monoclinic space groups *Cc* and *C*2/*c*. It was later determined that the centrosymmetric space group *C*2/*c* was correct. The structure was solved by direct methods and refined on F^2 by full-matrix least-squares techniques. Hydrogen atoms were included using a riding model. The molecule was located about a 2-fold axis. There were two disordered toluene solvent molecules present that were included using multiple components with partial site-occupancy factors. Hydrogen atoms associated with the disordered solvent molecules were not included in the refinement. At convergence, wR2 = 0.1229 and GOF = 1.068 for 288 variables refined against 5774 data (0.80 Å). As a comparison for refinement on *F*, R1 = 0.0451 for those 4566 data with $I > 2.0\sigma(I)$.

(C$_5$Me$_4$H)$_3$Ce, 4. A light blue crystal of approximate dimensions 0.06 × 0.18 × 0.22 mm^3 was handled as described above. The systematic absences were consistent with the rhombohedral space groups *R*3 and $R\bar{3}$. It was later determined that the centrosymmetric space group $R\bar{3}$ was correct. The structure was solved by direct methods and refined on F^2 by full-matrix least-squares techniques. Hydrogen atoms were located from a difference map and refined (*x*, *y*, *z*, and U_{iso}). The molecule was located on a 3-fold rotation axis. At convergence, wR2 = 0.0395 and GOF = 1.121 for 138 variables refined against 1941 data. As a comparison for refinement on *F*, R1 = 0.0161 for those 1775 data with $I > 2.0\sigma(I)$. The structure was refined as a merohedral twin using the SHELXTL TWIN command (BASF = 0.2077).

(C$_5$Me$_4$H)$_3$Pr, 5. A yellow crystal of approximate dimensions 0.14 × 0.18 × 0.25 mm^3 was handled as described above. The systematic absences were consistent with the rhombohedral space groups *R*3 and $R\bar{3}$. It was later determined that the centrosymmetric space group $R\bar{3}$ was correct. The structure was solved by direct methods and refined on F^2 by full-matrix least-squares techniques. Hydrogen atoms were located from a difference map and refined (*x*, *y*, *z*, and U_{iso}). The molecule was located on a 3-fold rotation axis. At convergence, wR2 = 0.0315 and GOF = 1.211 for 138 variables refined against 1932 data. As a comparison for refinement on *F*, R1 = 0.0128 for those 1834 data with $I > 2.0\sigma(I)$. The structure was refined as a merohedral twin using the SHELXTL TWIN command (BASF = 0.4064).

[(C$_5$Me$_4$H)$_2$(THF)Ce]$_2$(μ-η^2:η^2-N$_2$), 6. A yellow crystal of approximate dimensions 0.11 × 0.19 × 0.28 mm^3 was handled as described above. The diffraction symmetry was 2/*m*, and the systematic absences were consistent with the monoclinic space groups *Cc* and *C*2/*c*. It was later determined that the centrosymmetric space group *C*2/*c* was correct. The structure was solved by direct methods and refined on F^2 by full-matrix least-squares techniques. Hydrogen atoms were included using a riding model. The molecule was located about a 2-fold rotation axis. There were two molecules of toluene solvent present per formula unit. At convergence, wR2 = 0.1001 and GOF = 1.077 for 297 variables refined against 6654 data. As a comparison for refinement on *F*, R1 = 0.0370 for those 4896 data with $I > 2.0\sigma(I)$.

[(C$_5$Me$_4$H)$_2$(THF)Pr]$_2$(μ-η^2:η^2-N$_2$), 7. A green crystal of approximate dimensions 0.17 × 0.19 × 0.35 mm^3 was handled as described above. The diffraction symmetry was 2/*m*, and the systematic absences were consistent with the monoclinic space groups *C*2, *Cm*, or *C*2/*m*. It was later determined that the noncentrosymmetric space group *C*2 was correct. The structure was solved by direct methods and refined on F^2 by full-matrix least-squares techniques. The molecule was located about a 2-fold rotation axis. Hydrogen atoms were included using a riding model. There were two molecules of toluene solvent present per formula unit. The solvent molecules were disordered and included using multiple components with partial site-occupancy factors. The tetramethylcyclopentadienyl ring defined by atoms C(10)−C(19) was also disordered. Atoms C(17A) and C(17B) were disordered over two positions. The site-occupancy factors of these two atoms were set to approximately 0.60 and 0.40, respectively, to account for the methyl carbon atom being disordered over the two positions. The ring-hydrogen atom associated with the disordered tetramethylcyclopentadienyl ligand could not be located and was not included in the refinement. At convergence, wR2 = 0.0964 and GOF = 1.136 for 155 variables refined against 6197 data (0.77 Å). As a comparison for refinement on *F*, R1 = 0.0366 for those 5802 data with $I > 2.0\sigma(I)$. Refinement of the model using the TWIN command or the Flack parameter[28] was inconclusive and yielded an absolute structure parameter of 0.50.

[(C$_5$Me$_5$)$_2$Ce]$_2$(μ-O), 8. Crystals of **8** were obtained from an attempted synthesis of **2**. A green crystal of approximate dimensions 0.05 × 0.20 × 0.20 mm^3 was handled as described above. The diffraction symmetry was 4/*mmm*, and the systematic absences were consistent with the tetragonal space group $I\bar{4}2m$, which was later determined to be correct. The structure was solved using the coordinates of an isomorphous lanthanum complex.[29] Hydrogen atoms were included using a riding model. At convergence, wR2 = 0.0417 and GOF = 1.112 for 59 variables refined against 1247 data. As a comparison for refinement on *F*, R1 = 0.0170 for those 1188 data with $I > 2.0\sigma(I)$. The structure was refined using the TWIN[26] command (BASF = 0.39(2)).

Results

Synthesis. 2 and **3** were made using the method previously reported for the lanthanum analog, [(C$_5$Me$_5$)$_2$(THF)La]$_2$(μ-η^2:η^2-N$_2$), **9**,[5] eq 3. The LnZ$_2$Z′/M (M = K, Na) method[5]

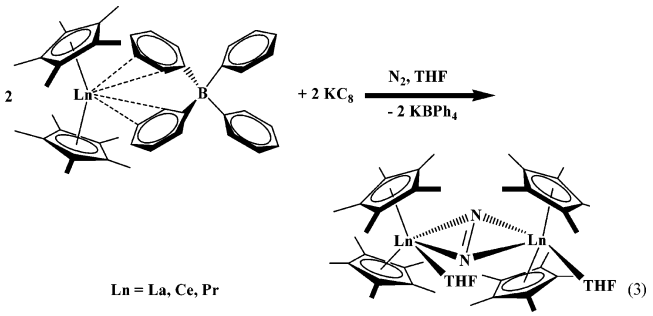

(3)

with [(C$_5$Me$_5$)$_2$Ln][(μ-Ph)$_2$BPh$_2$] precursors was used to obtain these complexes instead of the LnZ$_3$/M approach[3,4] with (C$_5$Me$_5$)$_3$Ln complexes[11] since the tetraphenylborate complexes are precursors to the (C$_5$Me$_5$)$_3$Ln compounds.

(28) Flack, H. D. *Acta. Crystallogr.* **1983**, *A39*, 876−881.
(29) Evans, W. J.; Davis, B. L.; Nyce, G. W.; Perotti, J. M.; Ziller, J. W. *J. Organomet. Chem.* **2003**, *677*, 89.

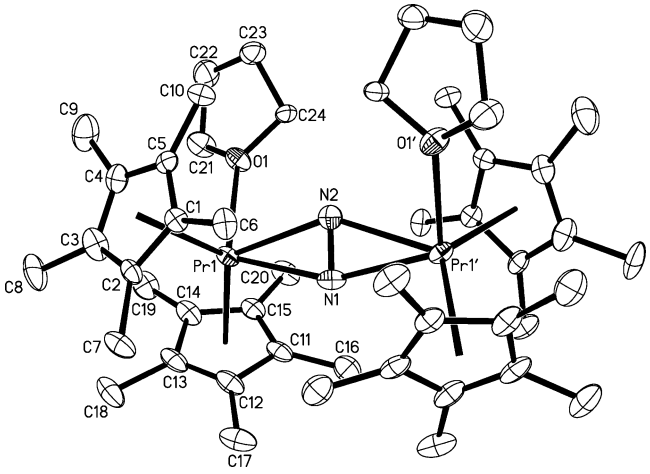

Figure 1. Thermal ellipsoid plot of $[(C_5Me_5)_2(THF)Pr]_2(\mu\text{-}\eta^2\text{:}\eta^2\text{-}N_2)$, **3**, with thermal ellipsoids drawn at the 50% probability level. The cerium analog, **2**, is isomorphous.

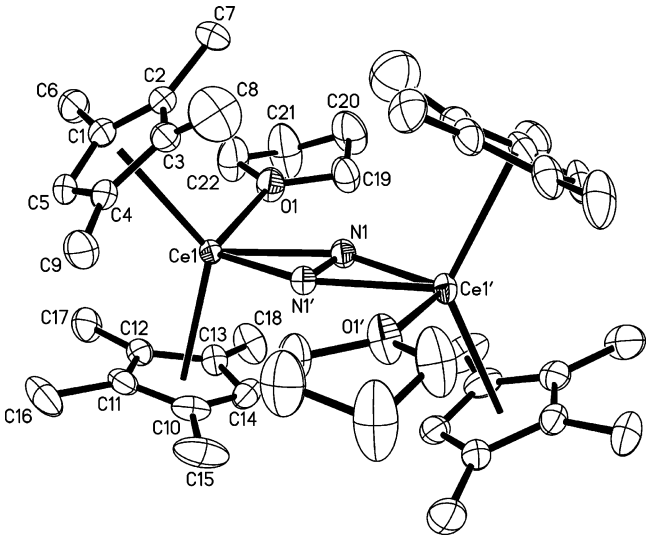

Figure 2. Thermal ellipsoid plot of $[(C_5Me_4H)_2(THF)Ce]_2(\mu\text{-}\eta^2\text{:}\eta^2\text{-}N_2)$, **6**, with thermal ellipsoids drawn at the 50% probability level.

Complexes **2** and **3** formed as dark red and yellow-orange thin needles, respectively, and were structurally characterized by X-ray crystallography, Figure 1.

6 and **7** were synthesized via the LnZ_3/M method, eq 4,

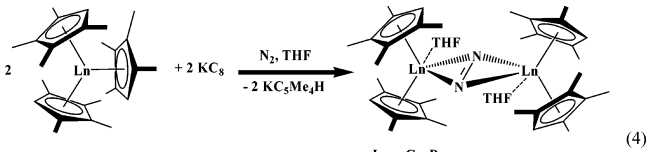

(4)

and identified by X-ray crystallography, Figure 2. The LnZ_3/M method was used in these cases since the $(C_5Me_4H)_3$-Ln (Ln = Ce, **4**; Pr, **5**, Figure 3) precursors can be made directly from $LnCl_3$ and KC_5Me_4H, eq 5. La[21] (**10**), Nd[22] (**11**), Sm[21] (**12**), Tb[21] (**13**), and Lu[6] (**14**) analogs of precursors **4** and **5** were previously reported, as were La (**15**)[5], Nd (**16**),[5] and Lu (**17**)[6] analogs of the reduced dinitrogen complexes **6** and **7**.

Complexes **6** and **7** were obtainable from excess sodium or potassium, as well as KC_8. Hence, the more weakly

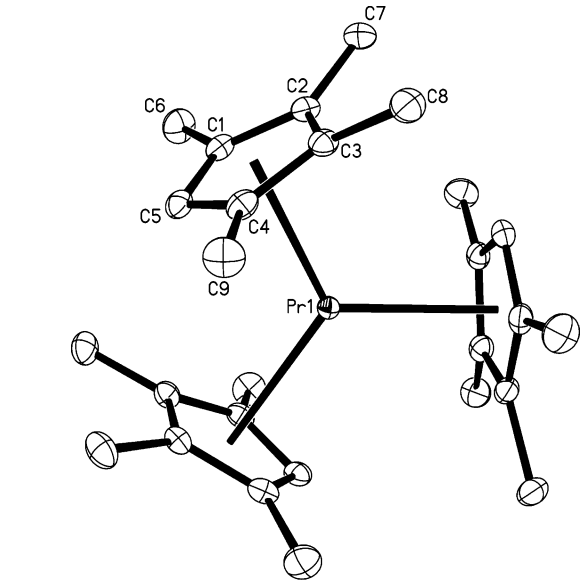

Figure 3. Thermal ellipsoid plot of $(C_5Me_4H)_3Pr$, **5**, with thermal ellipsoids drawn at the 50% probability level. The cerium analog, **4**, is isomorphous.

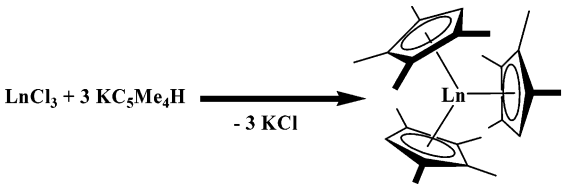

(5)

Ln = La, Ce, Pr, Nd, Sm, Tb, Lu

reducing sodium can be used in this LnZ_3/M reaction in a manner analogous to the $[(Me_3Si)_2N]_3Ln/M/N_2$ reduction system.[3,4] The colors of the $(C_5Me_4H)^{1-}$ complexes differ from those of the $(C_5Me_5)^{1-}$ complexes, **2** and **3**. Complex **6** crystallizes as bright yellow crystals, while **7** crystallizes as dark green crystals.

^{15}N NMR Spectra of Ce and Pr Complexes. ^{15}N analogs of **2**, **3**, **6**, and **7** were prepared from $^{15}N_2$. The ^{15}N NMR spectra of **2-^{15}N** and **6-^{15}N** showed singlets with 20−25 Hz half-height line widths[20] at 871 and 1001 ppm, respectively. To our knowledge, the only other reports of ^{15}N NMR data on cerium complexes are those reported for solutions of Ce^{3+} in the presence of $(^{15}NO_3)^{1-}$ [30] and $(^{15}NCS)^{1-}$ [31] counter ions. In those studies, the $^{15}NO_3^{1-}$ ion exhibited a shift of between −40 and −120 ppm compared to the sodium salt, whereas the $(^{15}NCS)^{1-}$ ion, which can bind directly via nitrogen to Ce^{3+}, was shifted between 450 and 550 ppm from the resonances for the sodium salt. The 450−550 ppm upfield shift of the thiocyanates is comparable to the difference between the resonances of **2-^{15}N** and **6-^{15}N** and the diamagnetic lanthanide $(N_2)^{2-}$ analogs recorded to date,[1,2−6] Table 2, which have resonances from 495 to 569 ppm.

The ^{15}N NMR spectra of the two ^{15}N-labeled praseodymium compounds, **3-^{15}N** and **7-^{15}N**, showed broad singlets

(30) Fratiello, A.; Kubo-Anderson, V.; Azimi, S.; Marinex, E.; Matejka, D.; Perrigan, R.; Yao, B. *J. Solution Chem.* **1992**, *21*, 651.
(31) Fratiello, A.; Kubo-Anderson, V.; Lee, D. J.; Perrigan, R. D.; Wong, K. *J. Solution Chem.* **1999**, *28*, 193.
(32) Fratiello, A.; Kubo-Anderson, V.; Azimi, S.; Chavez, O.; Laghaei, F.; Perrigan, R. D. *J. Solution Chem.* **1993**, *22*, 519.

Table 2. ^{15}N NMR Shifts of $[Z_2(THF)Ln]_2(\mu\text{-}\eta^2\text{:}\eta^2\text{-}N_2)$ Complexes

compound	^{15}N NMR shift (δ)[a]	ref
$\{[(Me_3Si)_2N]_2(THF)La\}_2(\mu\text{-}\eta^2\text{:}\eta^2\text{-}N_2)$	516	4
$\{[(Me_3Si)_2N]_2(THF)Y\}_2(\mu\text{-}\eta^2\text{:}\eta^2\text{-}N_2)$	513 (t)	3
$\{[(Me_3Si)_2N]_2(THF)Lu\}_2(\mu\text{-}\eta^2\text{:}\eta^2\text{-}N_2)$	557	3
$[(C_5Me_5)_2(THF)La]_2(\mu\text{-}\eta^2\text{:}\eta^2\text{-}N_2)$, **9**	569	5
$[(C_5Me_5)_2(THF)Ce]_2(\mu\text{-}\eta^2\text{:}\eta^2\text{-}N_2)$, **2**	871	this paper
$[(C_5Me_5)_2(THF)Pr]_2(\mu\text{-}\eta^2\text{:}\eta^2\text{-}N_2)$, **3**	2231	this paper
$[(C_5Me_4H)_2(THF)La]_2(\mu\text{-}\eta^2\text{:}\eta^2\text{-}N_2)$, **15**	495	5
$[(C_5Me_4H)_2(THF)Ce]_2(\mu\text{-}\eta^2\text{:}\eta^2\text{-}N_2)$, **6**	1001	this paper
$[(C_5Me_4H)_2(THF)Pr]_2(\mu\text{-}\eta^2\text{:}\eta^2\text{-}N_2)$, **7**	2383	this paper
$[(C_5Me_4H)_2(THF)Lu]_2(\mu\text{-}\eta^2\text{:}\eta^2\text{-}N_2)$, **17**	521	6

[a] All chemical shifts were measured using an external reference of ^{15}N-formamide.

at 2231 and 2383 ppm, respectively. Again, the only other reports of ^{15}N NMR data on praseodymium complexes are those reported for solutions containing the $(^{15}NO_3)^{1-}$ [32] and $(^{15}NCS)^{1-}$ [33] ions. As observed for Ce^{3+}, the ^{15}N resonances of the Pr^{3+} nitrate salts were shifted downfield, in this case -150 to -200 ppm, compared to the sodium salt and the thiocyanates were shifted upfield 1500 ppm for Pr^{3+}. As for the dinitrogen complexes **2-^{15}N** and **6-^{15}N**, the resonances of **3-^{15}N** and **7-^{15}N** were shifted upfield like the thiocyanates. The difference between the shifts of the paramagnetic Pr (2231−2383 ppm) and diamagnetic lanthanide (495−569 ppm) dinitrogen complexes was also like that of the thiocyanates (1500 ppm). Since Pr^{3+} has a higher magnetic moment, its dinitrogen complexes are expected to have larger shifts.

^{15}N NMR Spectra of $[(C_5Me_5)_2Sm]_2(\mu\text{-}\eta^2\text{:}\eta^2\text{-}N_2)$. Since **1** exists in a dynamic equilibrium in solution, ^{15}N-enriched **1** was generated in situ at low temperature. The formation of **1** upon lowering the temperature of $(C_5Me_5)_2Sm$ under N_2 has previously been monitored by ^1H and ^{13}C NMR spectroscopy.[10] At room temperature, the ^{15}N NMR spectra of $(C_5Me_5)_2Sm$ under $^{15}N_2$ showed only free $^{15}N_2$ at -75 ppm.[2,34] However, as the temperature was lowered to 263 K, a second peak appeared downfield at -117 ppm. As the temperature was lowered further, the ^{15}N resonance shifted downfield to -161 ppm at 203 K. There is a linear shift of the ^{15}N resonance between -117 and -161 K, Figure 4, of 0.7 ppm/K, with a correlation coefficient of 0.933. The shifting is reversible.

To our knowledge, only two other reports of ^{15}N NMR resonances in the presence of samarium are reported, again for the $(^{15}NO_3)^{1-}$ [35] and $(^{15}NCS)^{1-}$ [35,36] salts. $(^{15}NO_3)^{1-}$ in the presence of Sm^{3+} shifts downfield by ca. 10−20 ppm from the sodium salt. In contrast, the $(^{15}NCS)^{1-}$ ion shifts upfield from the sodium salt by about 250 ppm with a temperature dependence of 3−5 ppm/K, over the range of -115 to -125 K, attributed to residual ligand exchange.

Structural Studies. $(C_5Me_4H)_3Ln$ (Ln = Ce, Pr). In the course of preparing **6** and **7**, the precursors **4** and **5** were characterized by X-ray crystallography. Since the NMR spectra of highly symmetric paramagnetic species of this type are not very definitive, crystallographic data are often obtained to ensure the identity of the complex. The structural data are presented here first for comparison with the dinitrogen complexes later. **5** and **6** are isomorphous with all of the previously characterized $(C_5Me_4H)_3Ln$ complexes, Ln = La[21] (**10**), Nd[22] (**11**), Sm[21] (**12**), Tb[21] (**13**), and Lu[6] (**14**). The three $(C_5Me_4H)^{1-}$ ring centroids in each of these complexes define a trigonal planar geometry around the metal with 120° (C_5Me_4H ring centroid)−Ln−(C_5Me_4H ring centroid) angles. There is only one crystallographically independent $(C_5Me_4H)^{1-}$ ring in the structures. The bond distances vary from structure to structure in a regular way depending on the size of the metal. Table 3 shows the comparison of the Ce and Pr complexes whose trivalent nine-coordinate radii differ by 0.017 Å. The five Ln−C(ring) distances vary in the following way, as illustrated with data for **4**: the ring carbon sans methyl, C(5), is the closest (2.748(2) Å), the adjacent ring carbons, C(1) and C(4), are next (2.795(2) and 2.794(2) Å, respectively), and the remaining ring carbons, C(2) and C(3), are further away, (2.886(2) and 2.881(2) Å, respectively). Table 3 shows the analogous distances in **5**.

$[(C_5Me_4H)_2(THF)Ln]_2(\mu\text{-}\eta^2\text{:}\eta^2\text{-}N_2)$ (Ln = Ce, 6; Pr, 7). The structure of **6** will be discussed next, since like the $(C_5Me_4H)_3Ln$ complexes just discussed, it is similar to the other $(C_5Me_4H)^{1-}$ analogs that have been crystallographically characterized, Ln = La[5] (**15**), Nd[5] (**16**), and Lu[6] (**17**). Each of these complexes has a planar $Ln_2(\mu\text{-}\eta^2\text{:}\eta^2\text{-}N_2)$ arrangement involving a formally dianionic $(N_2)^{2-}$ ligand. This formerly rare mode of binding dinitrogen has become the signature structure of lanthanide dinitrogen complexes.[7] Complex **6** has a N−N distance of 1.235(6) Å that is consistent with the reduction of dinitrogen to $(N{=}N)^{2-}$,[37] Table 4.

In contrast to the $[(C_5Me_4H)_2(THF)Ln]_2(\mu\text{-}\eta^2\text{:}\eta^2\text{-}N_2)$ complexes discussed above, which all crystallize in the *C*2 space group, complex **7** crystallizes in the *C*2/*c* space group. This was found in two separate attempts to collect X-ray data. Although the data for **7** were sufficient to show that the atomic connectivity matched that of the other $[(C_5Me_4H)_2(THF)Ln]_2(\mu\text{-}\eta^2\text{:}\eta^2\text{-}N_2)$ complexes, the data were not good enough to provide reliable metrical information. Although this variation in space group is not common for lanthanides, structurally analogous lanthanide complexes do sometimes crystallize in different space groups.[38]

$[(C_5Me_5)_2(THF)Ln]_2(\mu\text{-}\eta^2\text{:}\eta^2\text{-}N_2)$, (Ln = Ce, 2; Pr, 3). Complexes **2** and **3** are isomorphous and have a planar $Ln_2(\mu\text{-}\eta^2\text{:}\eta^2\text{-}N_2)$ structure similar to other $[(Z)_2(THF)Ln]_2(\mu\text{-}\eta^2\text{:}\eta^2\text{-}N_2)$ complexes.[3−7,39] However, **2** and **3** both differ from

(33) Fratiello, A.; Kubo-Anderson, V.; Lee, R. A.; Patrick, M.; Perrigan, R. D.; Porras, T. R.; Sharp, A. K.; Wong, K. *J. Solution Chem.* **2001**, *30*, 77.

(34) (a) Grinter, R.; Mason, J. *J. Chem. Soc. A* **1970**, 2196. (b) Donovan-Mtunzi, S.; Richards, R. L. *J. Chem. Soc., Dalton Trans.* **1984**, 2429.

(35) Fratiello, A.; Kubo-Anderson, V.; Bolanos, E.; Chavez, O.; Laghaei, F.; Ortega, J. V.; Perrigan, R. D.; Reyes, F. *J. Solution Chem.* **1994**, *23*, 1019.

(36) Fratiello, A.; Kubo-Anderson, V.; Perrigan, R.; Wong, K. *J. Solution Chem.* **1998**, *27*, 581.

(37) Tables of Interatomic Distances and Configurations in Molecules and Ions. *Chemical Society Special Publications*; Sutton, L. E.; The Chemical Society: London, 1958; Vol. 11.

(38) Evans, W. J.; Giarikos, D. G.; Johnston, M. A.; Greci, M. A.; Ziller, J. W. *J. Chem. Soc. Dalton Trans.* **2002**, 520.

(39) Evans, W. J.; Zucchi, G.; Ziller, J. W. *J. Am. Chem. Soc.* **2003**, *125*, 10.

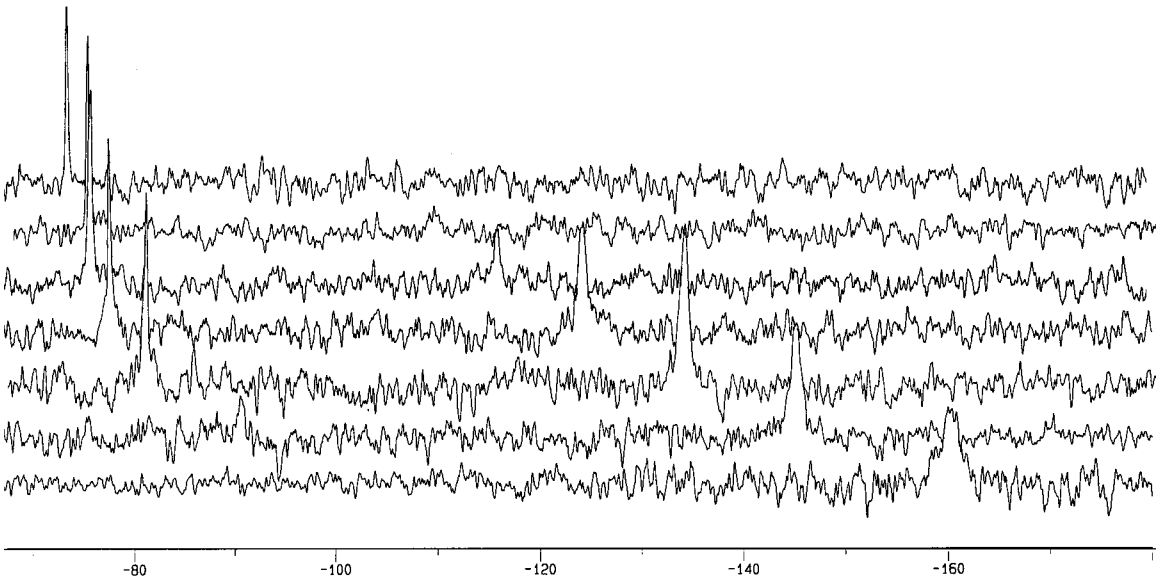

Figure 4. Variable-temperature ^{15}N NMR of $[(C_5Me_5)_2Sm]_2(\mu\text{-}\eta^2\text{:}\eta^2\text{-}^{15}N_2)$ at $T = 293, 278, 263, 248, 233, 218, 203$ K (top to bottom).

Table 3. Selected Bond Distances (Å) and Angles (deg) for $(C_5Me_4H)_3Ce$, **4** and $(C_5Me_4H)_3Pr$, **5**

compound	**4**	**5**
Ln(1)−Cnt	2.552	2.532
Ln(1)−C(1)	2.7949(18)	2.7733(17)
Ln(1)−C(2)	2.8861(18)	2.868
Ln(1)−C(3)	2.8807(18)	2.8642(18)
Ln(1)−C(4)	2.7939(18)	2.7768(17)
Ln(1)−C(5)	2.7483(17)	2.7283(14)
Cnt−Ln(1)−Cnt	120	120

Table 4. Selected Bond Distances (Å) and Angles (deg) for $[(C_5Me_4H)_2(THF)Ce]_2(\mu\text{-}\eta^2\text{:}\eta^2\text{-}N_2)$, **6**

Ce(1)−Cnt1	2.551	Ce(1)−C(11)	2.834(4)
Ce(1)−Cnt2	2.543	Ce(1)−C(12)	2.836(4)
Ce(1)−C(1)	2.863(4)	Ce(1)−C(13)	2.818(4)
Ce(1)−C(2)	2.845(4)	Ce(1)−C(14)	2.779(4)
Ce(1)−C(3)	2.786(4)	Ce(1)−N(1)	2.475(3)
Ce(1)−C(4)	2.776(4)	Ce(1)−N(1′)	2.428(3)
Ce(1)−C(5)	2.834(4)	Ce(1)−O(1)	2.589(3)
Ce(1)−C(10)	2.798(4)	N(1)−N(1′)	1.235(6)
Cnt1−Ce(1)−Cnt2	130.1	Ce(1)−N(1)−Ce(1′)	150.73(14)
Cnt1−Ce(1)−O(1)	103.4	N(1)−Ce(1)−N(1′)	29.16(14)
Cnt2−Ce(1)−O(1)	104.6		

the other complexes in that the THF molecules in **2** and **3** are in a cis arrangement, Figure 5. In contrast, the five $[(C_5Me_4H)_2(THF)Ln]_2(\mu\text{-}\eta^2\text{:}\eta^2\text{-}N_2)$[5,6] and nine $\{[(Me_3Si)_2N]_2(THF)Ln\}_2(\mu\text{-}\eta^2\text{:}\eta^2\text{-}N_2)$[3,4,39] complexes crystallographically characterized to date have a trans arrangement of THF ligands. A similar cis arrangement was found in the lanthanum analog **9**,[5] Table 5, although **9** crystallizes in a different space group, $P2_1/c$, than that of **2** and **3**, $C2/c$. Despite the difference in space groups, **2**, **3**, and **9** exhibit similar metrical parameters. The Ln−O(THF) distances in **2** (2.607(4) Å), **3** (2.595(4) Å), and **9** (2.630(3) Å) and the Ln−Cnt distances in **2** (2.575 and 2.580 Å), **3** (2.566 and 2.548 Å), and **9** (2.614 and 2.604 Å) are equivalent when they are adjusted for differences in ionic radius.[40] The O(THF)−Ln···Ln−O(THF) torsional angles for **2** (70.03°), **3** (70.26°), and **9** (71.30°) are also similar. In contrast, the analogous torsional angle in **6** is 167.45°.

Another difference between the $[(C_5Me_5)_2(THF)Ln]_2(\mu\text{-}\eta^2\text{:}\eta^2\text{-}N_2)$ complexes, **2**, **3**, and **9**, and the other previously characterized $[(Z)_2(THF)Ln]_2(\mu\text{-}\eta^2\text{:}\eta^2\text{-}N_2)$ complexes ($Z = C_5Me_4H$,[5,6] $N(SiMe_3)_2$[3,4,39]) is that the nitrogen atoms in the $(N_2)^{2-}$ ligand in **2**, **3**, and **9** are not crystallographically equivalent. They are symmetry-related in the other structures. The N−N distances in **2**, **3**, and **9**, 1.258(9), 1.242(9), and 1.233(5) Å, respectively, are consistent with the reduction of dinitrogen to $(N{=}N)^{2-}$[37] and are similar to those in the other complexes. However, the Ln−N distances in **2**, **3**, and **9** span a wider range than those found in the $(N_2)^{2-}$ complexes with symmetry-equivalent nitrogen atoms. These Ln−N distances are 2.478(4) and 2.537(4) Å for **9**, 2.455(2) and 2.524(2) Å for **2**, and 2.446(1) and 2.512(2) Å for **3**. In comparison, the Ln−N distances in $\{[(Me_3Si)_2N]_2(THF)Ln\}_2(\mu\text{-}\eta^2\text{:}\eta^2\text{-}N_2)$ are at most 0.031 Å different in nine different examples. The angles are also disparate: Ln1−N1−Ln1′ and Ln1−N2−Ln1′ angles are, respectively, 157.3(2)° and 145.8(2)° in **9**, 156.9(3)° and 144.7(3)° in **2**, and 157.0(3)° and 145.1(3)° in **3**. In contrast, the $\{[(Me_3Si)_2N]_2(THF)Ln]_2(\mu\text{-}\eta^2\text{:}\eta^2\text{-}N_2)$ complexes have a single Ln−N−Ln′ angle and all fall in the range of 146.9(1)−149.4(1)°. As a result of the unsymmetrical Ln−N−Ln′ angles in **2**, **3**, and **9**, the $(N_2)^{2-}$ ligand does not lie symmetrically between the lanthanide ions in the Ln_2N_2 plane, Figure 5. It is located to one side of the plane, as shown in the top view in Figure 6 and this puts it closer to the THF molecules. This variation in structure reflects the flexibility in the coordination sphere of lanthanide complexes. It is likely that in solution these asymmetries are not maintained.

$[(C_5Me_5)_2Ce]_2(\mu\text{-}O)$. Crystals of **8**, Figure 7, Table 6, were obtained in one synthesis of **2**. The presence of oxide might indicate the relatively high reactivity of the dinitrogen species,[11,41] but oxide products are known to arise despite attempts to rigorously exclude air and water.[42,43]

(40) Shannon, R. D. *Acta Crystallogr.* **1976**, *A 32*, 751.

(41) Evans, W. J.; Davis, B. L.; Ziller, J. W. *Inorg. Chem.* **2001**, *40*, 6341.
(42) Evans, W. J.; Kozimor, S. A.; Ziller, J. W. *Polyhedron* **2004**, *23*, 2689.

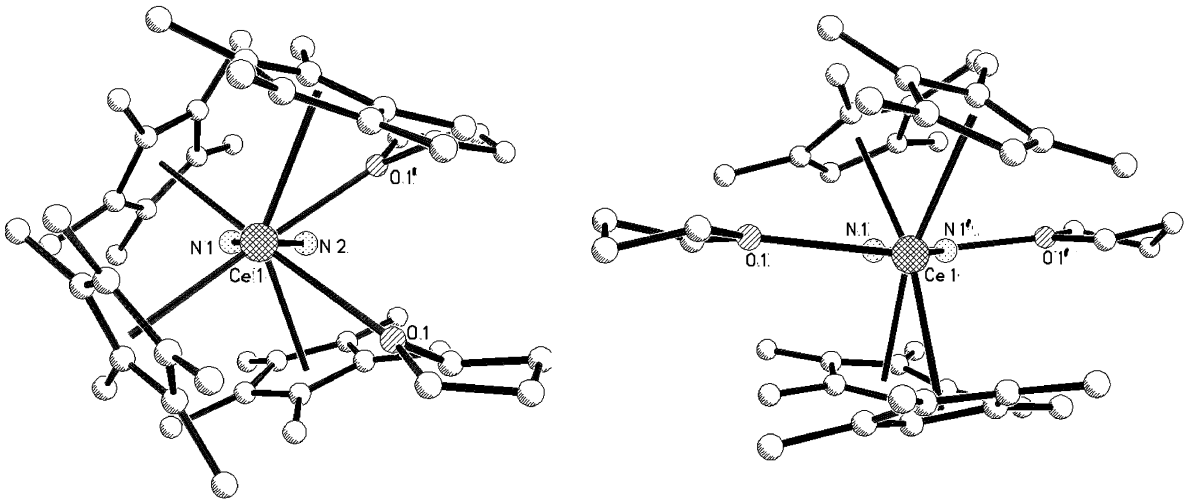

Figure 5. Ball and stick plot of $[(C_5Me_5)_2(THF)Ce]_2(\mu\text{-}\eta^2\text{:}\eta^2\text{-}N_2)$, **2**, and $[(C_5Me_4H)_2(THF)Ce]_2(\mu\text{-}\eta^2\text{:}\eta^2\text{-}N_2)$, **6** as seen down the Ce···Ce axes.

Table 5. Selected Bond Distances (Å) and Angles (deg) for $[(C_5Me_5)_2(THF)La]_2(\mu\text{-}\eta^2\text{:}\eta^2\text{-}N_2)$,[5] **9**, $[(C_5Me_5)_2(THF)Ce]_2(\mu\text{-}\eta^2\text{:}\eta^2\text{-}N_2)$, **2**, and $[(C_5Me_5)_2(THF)Ce]_2(\mu\text{-}\eta^2\text{:}\eta^2\text{-}N_2)$, **3**

compound	**9**[a]	**2**	**3**
Ln(1)−Cnt(1)	2.614	2.575	2.566
Ln(1)−Cnt(2)	2.604	2.580	2.548
Ln(1)−C(1)	2.877(5)	2.827(5)	2.801(5)
Ln(1)−C(2)	2.866(4)	2.831(6)	2.818(5)
Ln(1)−C(3)	2.901(5)	2.875(5)	2.859(6)
Ln(1)−C(4)	2.895(5)	2.852(5)	2.866(6)
Ln(1)−C(5)	2.873(5)	2.835(5)	2.829(5)
Ln(1)−C(11)	2.854(5)	2.826(5)	2.798(5)
Ln(1)−C(12)	2.860(5)	2.834(5)	2.809(6)
Ln(1)−C(13)	2.881(5)	2.868(5)	2.854(5)
Ln(1)−C(14)	2.884(5)	2.873(5)	2.832(5)
Ln(1)−C(15)	2.870(5)	2.844(5)	2.806(5)
Ln(1)−O(1)	2.636(3)	2.607(4)	2.595(4)
Ln(1)−N(1)	2.537(4)	2.4548(15)	2.4459(14)
Ln(1)−N(2)	2.478(4)	2.524(2)	2.512(2)
N(1)−N(2)	1.233(5)	1.258(9)	1.242(9)
Cnt(1)−Ln(1)−Cnt(2)	128.8	131.3	130.7
Cnt(1)−Ln(1)−O(1)	102.5	101.7	100.3
Cnt(2)−Ln(1)−O(1)	101.8	100.4	101.7
Ln(1)−N(1)−Ln(1′)	145.77(16)	156.9(3)	157.0(3)
Ln(1)−N(2)−Ln(1′)	157.33(18)	144.7(3)	145.1(3)
N(1)−Ln(1)−N(2)	28.43(12)	29.2(2)	29.0(2)
O(1)−Ln(1)···Ln(1′)−O(1′)	71.30	70.03	70.26

[a] For **9**, there are two independent atoms of La per molecule, La(1) and La(2). Since the La(1) and La(2) distances and angles are comparable only those of La(1) are given here, Ln(1′) in the table refers to La(2) in **9**.

Complex **8** is isomorphous with other unsolvated pentamethylcyclopentadienyl lanthanide oxides $[(C_5Me_5)_2Ln]_2(\mu\text{-O})$ (Ln = La[29] (**18**), Nd[44] (**19**), Sm[45] (**20**), and Y[46] (**21**)). The Ce(1)−O(1)−Ce(1′) angle is linear, and the metrical parameters of the metallocene unit are similar to the other analogs when the differences in ionic radii are taken into account.[40] For example, the 2.534 Å Ce−(C_5Me_5 ring centroid) distance is similar to the radius normalized values[40] in the other examples: 2.544 Å for **18**, 2.530 for **19**, 2.534 for **20**, and 2.520 Å for **21.** There is also reasonably close agreement between the 2.1405(3) Å Ce−O distance and the radius normalized analogs: 2.127 Å for **18**, 2.135 Å for **19**, 2.158 Å for **20**, and 2.177 Å in **21**.

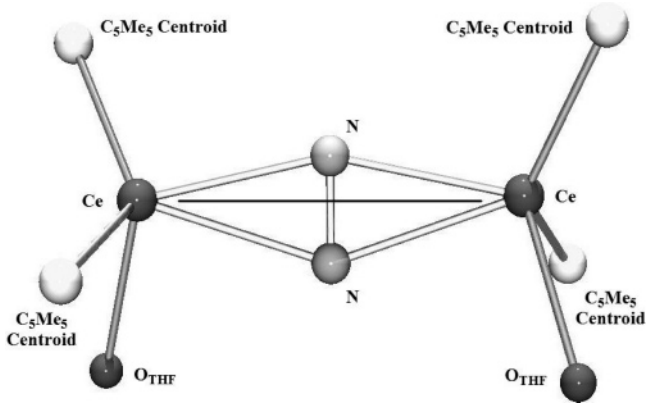

Figure 6. Ball and stick plot of the central $Ce_2(\mu\text{-}\eta^2\text{:}\eta^2\text{-}N_2)$ moiety in **2** as seen from the top of the $Ce_2(\mu\text{-}\eta^2\text{:}\eta^2\text{-}N_2)$ plane. The THF oxygen atoms and the C_5Me_5 ring centroids are also included. A line has been drawn between the cerium atoms to show the asymmetry.

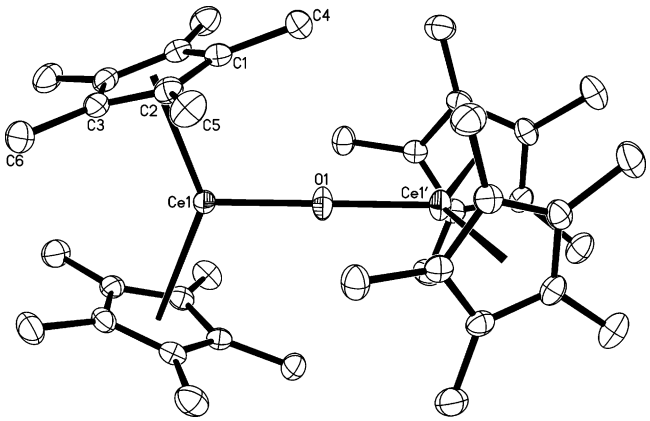

Figure 7. Thermal ellipsoid plot of $[(C_5Me_5)_2Ce]_2(\mu\text{-O})$, **8**, with thermal ellipsoids drawn at the 50% probability level.

(43) (a) Lin, G.; Wong, W.-T. *Polyhedron* **1995**, *14*, 3167. (b) Deacon, G. B.; Fallon, G. D.; Forsyth, C. M.; Gatehouse, B. M.; Junk, P. C.; Philosof, A.; White, P. A. *J. Organomet. Chem.* **1998**, *565*, 201. (c) P. Roussel, P.; Boaretto, R.; Kingsley, A. J.; Alcock, N. W. Scott, P. *J. Chem. Soc., Dalton. Trans.* **2002**, 1423. (d) Evans, W. J.; Davis, B. L.; Nyce, G. W.; Perotti, J. M.; Ziller, J. W. *J. Organomet. Chem.* **2003**, *677*, 89. (e) Karmazin, L.; Mazzanti, M.; Pécaut, J. *Inorg. Chem.* **2003**, *42*, 5900.

(44) Tilley, T. D.; Rheingold, A. L.; Allen, M. B. Private Communication to the CCDC, 1996.

(45) Evans, W. J.; Grate, J. W.; Bloom, I.; Hunter, W. E.; Atwood, J. L. *J. Am. Chem. Soc.* **1985**, *107*, 405.

(46) Ringelberg, S. N.; Meetsma, A.; Troyanov, S. I.; Hessen, B.; Teuben, J. H. *Organometallics* **2002**, *21*, 1759.

Table 6. Selected Bond Distances (Å) and Angles (deg) for $[(C_5Me_5)_2Ce]_2(\mu\text{-O})$, **8**

Ce(1)−Cnt	2.534	Ce(1)−C(3)	2.826(2)
Ce(1)−C(1)	2.789(3)	Ce(1)−O(1)	2.1405(3)
Ce(1)−C(2)	2.793(2)		
Cnt−Ce(1)−O(1)	110.3	Cnt−Ce(1)−Cnt	139.4

The structure of complex **8** differs significantly from that of the solvated $[(C_5Me_5)_2(THF)Ce]_2(\mu\text{-O})$,[47] **22**. As expected for a higher-coordinate complex, the solvated complex has slightly longer Ce−(C_5Me_5 ring centroid) distances, 2.588(3) and 2.604(3) Å, and Ce−O(oxide) lengths, 2.183(5) and 2.185(4) Å. In addition, it has a nonlinear Ce−O−Ce angle of 175.9(2)°.

Discussion

The successful use of the LnZ_3/M and LnZ_2Z'/M reductive methods with the precursors $[(C_5Me_5)_2Ce][(\mu\text{-Ph})_2BPh_2]$ and **4** via eqs 3 and 4, respectively, has provided the first crystallographically characterizable reduced dinitrogen complexes of cerium. Similarly, using $[(C_5Me_5)_2Pr][(\mu\text{-Ph})_2BPh_2]$ and **5** as precursors, examples of reduced dinitrogen complexes of praseodymium have been obtained. In contrast, attempts to accomplish dinitrogen reduction with Ce and Pr using the $[(Me_3Si)_2N]_3Ln$/M reduction system did not generate crystallographically characterizable complexes for these metals. Only $\{Ln[N(SiMe_3)_2]_4\}^{1-}$ products, presumably formed from the $Ln[N(SiMe_3)_2]_3$ precursor and $KN(SiMe_3)_2$ byproduct, were isolated. The results reported here show that there was nothing unusual about Ce and Pr that prevented formation of $Ln_2(\mu\text{-}\eta^2\text{:}\eta^2\text{-}N_2)$ complexes if the appropriate Z ligand was present.

With the synthesis of the new complexes discussed here, reduced dinitrogen complexes have been crystallographically characterized for all the lanthanides except for radioactive Pm and the two most readily reducible trivalent ions Eu^{3+} and Yb^{3+}. The $(N_2)^{2-}$ ligand is likely to be sufficiently reducing to convert Eu^{3+} and Yb^{3+} to their divalent ions and N_2.

The ^{15}N NMR studies of the Ce and Pr dinitrogen complexes show that ^{15}N NMR data are obtainable on these paramagnetic systems. The shifts are substantial, however, even for these lanthanide ions that have relatively low magnetic moments. In fact, there was difficulty in initially finding the resonances. Given the challenges in collecting these data, this is clearly not a routine characterization technique. However, it does unequivocally show the presence of complexes of dinitrogen.

The temperature-dependent ^{15}N data on **1** are consistent with the equilibrium observed earlier by ^1H and ^{13}C NMR spectroscopy. Due to the accessibility of the Sm^{2+} oxidation state, this dinitrogen reduction is reversible. In this sense, it is the crossover point between Eu^{2+} and Yb^{2+}, which are too weak to reduce dinitrogen, and the other lanthanides that do not revert to Ln^{2+} complexes once the $(Ln^{3+})_2/(N_2)^{2-}$ complex has formed.

The structural data obtained on **4**, **5**, **6**, and **8** were conventional. These complexes had structures and metrical parameters as expected based on analogues in the literature. This is typical of lanthanide complexes since the 4f valence orbitals have a limited radial extension and the $4f^n$ electron configuration generally does not affect structure.

The structures of **2** and **3**, however, show a new aspect of lanthanide dinitrogen chemistry and the planar $Ln_2(\mu\text{-}\eta^2\text{:}\eta^2\text{-}N_2)$ unit. In these complexes, the $(N_2)^{2-}$ ligand is skewed to one side in the plane. Also asymmetric in these structures is the location of the THF molecules of solvation. This readily accessible variation in structure is also consistent with the fact that the valence orbitals of these ions are not heavily involved in generating the structures. Evidently, there is considerable flexibility in how the $(N_2)^{2-}$ ion binds to two $[Z_2Ln(THF)]^{1+}$ moieties. As a compact, two-donor-atom, dianionic ligand, the $(N_2)^{2-}$ ion constitutes a powerful ligating moiety for binding two lanthanide ions together. This ion apparently has an additional advantage in that it can bind asymmetrically, as well as symmetrically, to the two electropositive centers. The consequences of this structural variation in reactivity remain to be determined.

Conclusion

The synthetic results reported here demonstrate that the LnZ_3/M and LnZ_2Z'/M reduction systems apply to Ce and Pr, as well as the other lanthanides. Reduced dinitrogen complexes are now known for all of the nonradioactive lanthanides except the most easily reduced Eu and Yb. The structures of **2** and **3** demonstrate how a slight change in the ancillary ligand, Z, can change the solid-state structure of the $[Z_2(THF)Ln]_2(\mu\text{-}\eta^2\text{:}\eta^2\text{-}N_2)$ complexes. The first ^{15}N NMR spectra of paramagnetic reduced dinitrogen lanthanide complexes have been obtained and demonstrate that ^{15}N NMR spectroscopy can be used to characterize paramagnetic lanthanide dinitrogen complexes.

Acknowledgment. We thank the National Science Foundation for support and Dr. Phillip Dennison for assistance in acquiring the ^{15}N NMR spectra and the magnetic susceptibility measurements.

Supporting Information Available: X-ray diffraction details (CIF) and X-ray data collection, structure solution, and refinement of compounds **2**−**8** (PDF). This material is available free of charge via the Internet at http://pubs.acs.org.

IC061485G

(47) Deelman, B.-J.; Booij, M.; Meetsma, A.; Teuben, J. H.; Kooijman, H.; Spek, A. L. *Organometallics* **1995**, *14*, 2306.